JOURNAL OF AIRCRAFT
Vol. 42, No. 6, November–December 2005

Vortex-Generator Model and Its Application to Flow Control

Adam Jirásek*
Swedish Defence Research Agency FOI, SE-172 90 Stockholm, Sweden

A new vortex-generator model is introduced, the jBAY model, which provides an efficient method for computational-fluid-dynamics (CFD) simulation of flow systems with vortex-generator arrays. The jBAY model is based on the lifting force theory of Bender, Anderson, and Yagle (Bender, E. E., Anderson, B. H., and Yagle, P. J., "Vortex Generator Modelling for Navier–Stokes Codes," American Society of Mechanical Engineers, FEDSM 99-6919, New York, July 1999) but uses a novel technique for defining the model control points. This greatly simplifies usage of the model as well as improving its performance and accuracy. The jBAY model is described in the context of its implementation in the CFD code Edge, an unstructured Reynolds-averaged Navier–Stokes solver. Results are presented for a single vortex generator on a flat plate and two flow control cases: an S-duct air intake and a high-lift wing configuration. The model is shown to give good agreement with both experimental results and with CFD computations where the vortex generator is fully gridded. It is demonstrated that the jBAY model is simple to apply and efficiently captures the effect of vortex generator arrays for both internal and external flows.

Nomenclature

$\boldsymbol{b}$	=	unit vector in the direction of the span of the vortex generator
C_{VG}	=	model constant
DC_{60}	=	pressure distortion index
E	=	energy
$\boldsymbol{F}_E$	=	inviscid and viscous fluxes in energy equation
$\boldsymbol{F}_M$	=	inviscid and viscous fluxes in momentum equations
$\boldsymbol{L}_i$	=	vortex-generator source term
M	=	Mach number
$\boldsymbol{n}$	=	unit vector normal to vortex-generator planform
Re	=	Reynolds number
S_{VG}	=	vortex-generator area
$\boldsymbol{t}$	=	unit vector tangential to the vortex generator planform and normal to $\boldsymbol{b}$
$\boldsymbol{u}$	=	velocity vector
α_∞	=	freestream angle of attack
Δt	=	time step
ΔV_i	=	mesh cell volume
ΔV_m	=	sum of volumes of cells where the vortex-generator source term is added
ρ	=	density

I. Introduction

VORTEX generators are highly efficient aerodynamic devices used widely in both external and internal aerodynamics as means of flow control.[1–8] They are local geometrical imperfections that cause the formation of longitudinal vortices giving rise to local mixing of the flow, energizing the boundary layer and consequently delaying or preventing separation or inducing secondary flow motion, which restructures the entire flowfield. The geometrical characteristics of vortex generators, as well as the characteristics of vortex generator installation, strongly depend both on the flow characteristics and on the type of problem. It is therefore desirable to use advanced computational-fluid-dynamics (CFD) methods, combined with experimental results and with statistical methods (for example, design of experiment) in order to find the best vortex-generator installation. Such an installation should be both efficient and insensitive to changes in the flow. This process is usually very time consuming. From a CFD point of view, the biggest problem connected with vortex generators is the amount of time required to generate grids around the vortex generators and the large number of grid points required to obtain an accurate solution. One way to overcome this difficulty is to model the vortex-generator effect, thus removing the need to grid the geometry of each individual vortex generator. According to May,[9] there are two types of vortex-generator models—the vortex-source model and the lifting-force model.

The vortex-source model constructs the source term based on either adding a specific circulation Γ or by adding another source term that is based on the velocity induced by this specific circulation according to the Biot–Savart law. The vorticity or other source term is usually added to the system of flow governing equations at the plane normal to the vector of vorticity at the vortex generator position. The key problem with this kind of model is that initial circulation Γ must be known. Research effort in this area aims at defining this specific circulation as well as other characteristics of circulation-induced vorticity.[4,9–12] The model must be combined with an appropriate boundary condition, which on a wall usually is a mirror vortex boundary condition.

The newer lifting-force model was developed by Bender et al. in 1999.[13] It is based on adding the lift force induced by the vortex generator to the system of Navier–Stokes equations. This lifting force spins the flow giving rise to the formation of vortices. In the model, the lift force is estimated from the Prandtl lifting theory. This model has attracted a great deal of interest, particularly in the United States. The model has been validated for flow over a flat plate with a single vortex generator. Detailed experiment and fully gridded analysis have been carried out providing validation and verification of the model.[2,6,13,14] More complex flow as the flows through the RAE M2129 S-duct have also been computed.[13] The model has, however, some limitations. In particular, it is difficult to define the points in the computational mesh where the vortex generator model should be applied. One serious consequence of this is that the model is not able to accurately model the combined effect of multiple vortex generators.

The lifting-force model is the more promising of the two vortex-generator models described here because it does not need estimates of any specific user input parameters. It is therefore this model that was chosen as the basis for development of the modified vortex-generator model.

II. Vortex-Generator Model

A. Bender–Anderson–Yagle Model

The vortex-generator model, which has been developed for the Edge CFD code,[15] is based on the model developed by Bender et al.[13]

Received 13 July 2004; presented as Paper 2004-4965 at the 22nd Applied Aerodynamics Conference and Exhibit, Providence, RI, 16–19 August 2004; revision received 14 October 2004; accepted for publication 14 October 2004.

*Research Engineer, The Aeronautics Division FFA. Member AIAA.

Fig. 1 Deviation of flow caused by vortex generator.

in which the generated vorticity is induced by a lateral force that is dependent on local flow quantities and the vortex-generator shape. The source term and its derivation, as written in the original article of Bender et al., is repeated here for completeness:

$$\Delta V_i \frac{\Delta \rho \boldsymbol{u}_i}{\Delta t} = \sum_j \boldsymbol{F}_M \Delta S + \boldsymbol{L}_i \tag{1}$$

$$\Delta V_i \frac{\Delta \rho E}{\Delta t} = \sum_j \boldsymbol{F}_E \Delta S + \boldsymbol{u}_i \boldsymbol{L}_i \tag{2}$$

The source term $\boldsymbol{L}_i$ is a function of the lifting force caused by the vortex generator and is corrected for losses caused by deviation of the flow from the vortex-generator surface. This side force is approximated by

$$\boldsymbol{L}_i = C_{\mathrm{VG}} S_{\mathrm{VG}} (\Delta V_i / V_m) \alpha \rho u^2 \boldsymbol{l} \tag{3}$$

where S_{VG} is the planparallel area of vortex generator, ΔV_i is the volume of the cell where the force is calculated, V_m is the sum of volumes of cells where the force term is applied, α is the angle of local velocity $\boldsymbol{u}$ to the vortex generator, and $\boldsymbol{l}$ is the unit vector on which the side force acts. The side force then acts so as to align the local velocity with the vortex generator (Fig. 1). The constant C_{VG} is a relaxation parameter which controls the strength of the side force [Eq. (3)] and consequently the intensity with which the local velocities align with the vortex generator. Theoretically, the constant C_{VG} could be set to infinity, and the velocity in the mesh points where the local force $\boldsymbol{L}_i$ is applied would then be perfectly align with a vortex generator ($\alpha \to 0$). At this point the local angle of attack $\alpha = 0$ and the model would become independent of the constant C_{VG}. However, for numerical reasons a finite value must be used. As long as the model constant is sufficiently large, the side force $\boldsymbol{L}_i$ will remain independent of C_{VG}.

Using a small angle approximation, we have

$$\boldsymbol{l} = \boldsymbol{u}/|\boldsymbol{u}| \times \boldsymbol{b} \tag{4}$$

$$\alpha \approx \boldsymbol{u} \cdot \boldsymbol{n}/|\boldsymbol{u}| \tag{5}$$

The final equation is multiplied by the term $\boldsymbol{u} \cdot \boldsymbol{t}/|\boldsymbol{u}|$, which represents losses of side force due to high angles of attack. The final expression for the side force according to Bender et al.[13] is as follows:

$$\boldsymbol{L}_i = C_{\mathrm{VG}} S_{\mathrm{VG}} (\Delta V_i / V_m) \rho (\boldsymbol{u} \cdot \boldsymbol{n})(\boldsymbol{u} \times \boldsymbol{b})(\boldsymbol{u} \cdot \boldsymbol{t}/|\boldsymbol{u}|) \tag{6}$$

The original Bender–Anderson–Yagle (BAY) model was applied in cells that were enclosed by the vortex geometry. For this case the user inputs are the position and orientation of the vortex generator, vectors ($\boldsymbol{t}, \boldsymbol{b}, \boldsymbol{n}$), and the vortex-generator model constant C_{VG}. According to Bender et al.,[13] the vortex-generator model can operate in two modes—asymptotic and linear. If the model is applied locally, such that the sum of the volumes V_m is close to the volume of vortex generator, then the model is in the so-called asymptotic mode and is insensitive to C_{VG}. Typically $C_{\mathrm{VG}} \approx 5$ and higher. If V_m differs substantially from the volume of the vortex generator (as in the case of a row of vortex generators), the model behaves in linear mode and is dependent on the constant C_{VG}. This model definition presents two difficulties. First, points laying inside the vortex generator must be defined, which might be a problem because most vortex generators are flat plates with almost negligible thickness. Second, the dependency of the model constant C_{VG} on vortex-generator installation when using the model in linear mode might be difficult to define. All of this makes the BAY model, to a certain extent, grid dependent.

To overcome the problem with definition of grid points laying inside the very thin vortex generators, Bender et al. during their study of the RAE M2129 channel proposed to treat the row of corotating vanes as one large vortex generator and to apply the source term at every mesh point in this pseudo vortex generator, thus creating a single vortex generator. Their approach led to results that are in good agreement with experimental data. However, the uncertainty of the model constant remains. Another question connected with this simplification is that, although vortices from each vane remained unresolved, the secondary motion of flow was predicted well. However, in more complicated vane installations the simplification might be too restrictive and could lead to misinterpretation of the physical phenomena. For such cases it is desirable to resolve the individual vortex filaments.

B. jBAY Model

The new jBAY is a development from the BAY model. The motivation behind this new model in this study is to attempt to overcome the shortcomings of the original BAY model, mainly to simplify the definition of points where the side force is calculated and extend the ability of the model to treat systems of multiple vortex generators without any simplifications. The term jBAY is introduced to denote the modified BAY model.

The vortex generator is replaced by a mean surface with zero thickness (as in potential theory). Points where the side force is calculated are then determined by the intersection of this mean surface with grid edges. The values of velocity and density needed in the vortex-generator model source term are interpolated to these points from grid nodes, and the resulting side force is then redistributed back to the nodes and added to the flow equations. The expression for the side force is thus the same as defined in the original model [Eqs. (3–6)].

Because the vortex generators are usually small plates glued to the wall, they are usually located entirely inside the boundary layer. In this region, the computational grid is sufficiently dense to ensure that vortex generator (VG) is surrounded by a fairly large number of neighboring nodes. This simplifies the search for appropriate points to define the vortex generator and allows the each vortex generator to be treated separately. It is, however, extremely important to keep in mind that sufficient grid resolution must be retained in order to resolve vortex filaments generated by the vortex generators. Because each vortex generator is defined locally by control points (that is, Sec. II.A), then the model is independent of the model constant C_{VG}. We note that another advantage of applying the model locally is that the source term which is added to the flow equations is applied in a very limited portion of the grid and hence reduces instabilities in the solution.

III. Edge CFD Code

The CFD flow solver used for this study is Edge,[15] a finite volume Navier–Stokes solver for unstructured meshes. It employs local time stepping, multigrid, and dual time stepping for steady-state and time-dependent problems. The data structure of the code is edge based so that the code is constructed as cell vertex. Edge can be run in parallel on a number of processors to efficiently solve large flow cases. It is equipped with a number of turbulence models based both on eddy-viscosity and explicit algebraic Reynolds-stress model (EARSM) assumption. The model that was used during this study was the two-equation k–ω model combined with Wallin and Johansson EARSM model[16] with compressible corrections. The source term in the vortex-generator model was calculated on the finest grid level in the first stage of the Runge–Kutta scheme and hence requires very little extra computational time. No underrelaxation was needed because all cases computed so far have been stable.

IV. Results

The jBAY vortex generator model has been used to calculate the flow over a flat plate with one subboundary-layer vortex generator. It has also been applied to the RAE M2129 S-duct test case with four different vortex-generator installations and to the flow

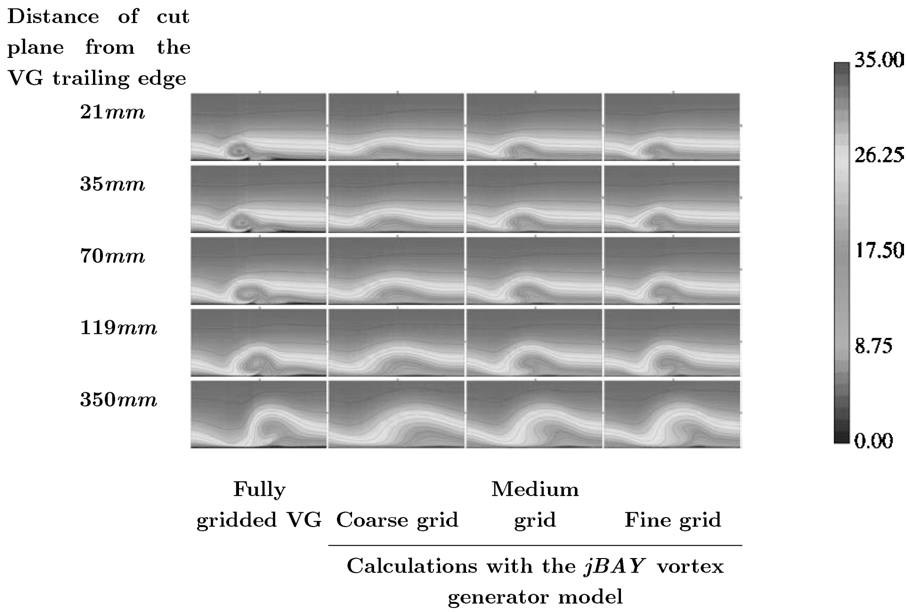

Fig. 2 Velocity contours in different cuts for vortex generated by the vortex generator on the flat plate.

over multi-element high-lift airfoil with vortex generators on a flap. Studies were carried out where both grid sensitivity as well as the sensitivity to the vortex generator model constant was tested.

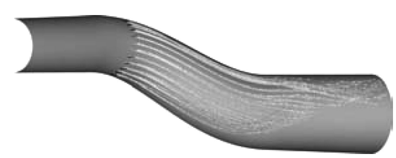

Fig. 3 Vortex filaments in flow through RAE M2129 S-duct.

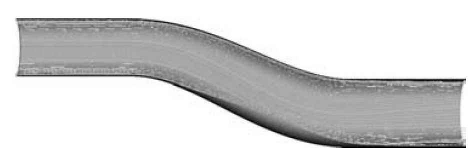

a) Baseline configuration

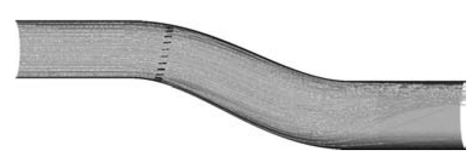

b) VG165 configuration—fully gridded VG

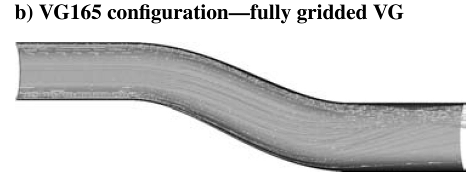

c) VG165 configuration—jBAY VG model

Fig. 4 Streamlines of flow through RAE M2129 S-duct.

A. Case 1: Single Vortex Generator on a Flat Plate

This test case is used to determine the ability of the jBAY vortex-generator model to capture the vorticity induced by a vortex generator on a flat plate. Both fully gridded computations and vortex-generator model calculations were carried out. The vortex generator is 7 mm high and 49 mm long and is mounted on a flat plate at a position where the thickness of the boundary layer is 45 mm. The angle of the vortex generator to the freestream velocity is $\alpha = 23$ deg, and the speed of flow is 34 m/s.

The grid for the fully gridded analysis was created using the grid generator Icem-Hexa and has approximately 700,000 cells. The quality of the grid on both the flat plate and the vortex generator is high, and the condition of $y^+ \approx 1$ is fulfilled. Three computational grids with different density of grid lines in spanwise direction were used for the calculation with the vortex-generator model. The medium grid has two times and the fine grid four times higher density of grid points in flat spanwise direction than the coarse grid. The grid density in streamwise and wall-normal direction of the flat was kept the same for all three grids. During this test, different model constants ($C_{\mathrm{VG}} = 7$ and 10) were used, but the differences were quite small; therefore, only the results for $C_{\mathrm{VG}} = 10$ are shown.

The effect of this refinement is clearly seen in Fig. 2, where velocity at five different cuts for all four test cases is plotted. This demonstrates the importance of having adequate grid density around the vortex generator for resolution of vorticity. When the density of grid lines is low, the vortex dissipates rather quickly, and its effect is underpredicted. As the grid density is increased, the patterns of the flowfield move closer to the patterns given by the fully gridded analysis.

It can be seen from Fig. 2 that the vortex-generator model was unable to model the core of a vortex where the velocities are around zero as shown in fully gridded solution. This is because of omission of viscous effects in the jBAY model. However, for the fine grid the effect on the flowfield is still reasonably close to that obtained from the fully gridded analysis.

B. Case 2: RAE M2129 S-Duct

The second test case used to validate the model was the flow through the RAE 2129 S-duct. This channel geometry is defined in Refs. 17 and 18. For this case, it is known from the experiments that at low Mach numbers the flow separates just after the first bend. The test had two goals: first to find out to which extent the model is independent of the value of the model constant C_{VG} and second to demonstrate the effectiveness of the vortex-generator model for the study of vortex-generator installation.

The purpose of the vortex-generator installation is to restructure the flowfield inside the S-duct by inducing secondary flow motion so that flow separation is reduced or completely prevented.[4] Figure 3 shows a perspective view of streamlines arising from the vortex generators demonstrating secondary motion. Figure 4 shows streamlines in the S-duct without and with vortex generators. The flow in the channel without vortex generators in Fig. 4a forms a "pocket" that represents separation. Figure 4b shows the same case of flow in S-duct with vortex generators. The difference between these two

Table 1 Geometrical features of different vortex-generator configurations

Designation	VG130	VG160	VG165	VG170
Number of VG pairs	11	13	11	11
Section location x/R_i	3	1	1	2
Blade height h/R_i	0.075	0.060	0.065	0.070
Chord length c/R_i	0.300	0.240	0.260	0.280
Spacing angle α_{vg}, deg	15	12.6	15	15
Angle of incidence β_{vg}, deg	16	16	16	16
Sector angle Θ_{vg}, deg	157.5	157.5	157.5	157.5

Table 2 DC_{60} for different C_{VG} constants in the AIP plane in flow through RAE M2129 S-duct

Designation	DC_{60}	Difference in %
Fully gridded	0.196	——
$C_{VG}=2$	0.110	−44.88
$C_{VG}=5$	0.173	−11.73
$C_{VG}=7$	0.182	−7.14
$C_{VG}=9$	0.187	−4.59
$C_{VG}=10$	0.188	−4.08
$C_{VG}=12$	0.191	−2.55

figures clearly shows the effectiveness of vortex generators as flow control devices. Finally, Fig. 4c shows the flow with model effect of vortex generators using jBAY model. The picture is very similar to the one with gridded vortex generators shown in Fig. 4b. This demonstrates that even for this complicated internal flow the jBAY model accurately reproduces the effect of the VG array.

The grid with fully gridded vortex generators was generated using Icem-Tetra and contains about 2.25 million points with prismatic layers on both the S-duct wall and on the vortex generators. The grid has an extension upstream of the inlet in order to build an adequate boundary layer on the walls of the S-duct and is also extended downstream of the outlet. The S-duct grid without vortex generators contains about 900,000 points and has been used for all other calculations except fully gridded computations. The size of the grid is thus reduced by a factor of 2.5 using the vortex-generator model. Taking account of the need to run fully gridded analysis in parallel, using jBAY model reduces the computation costs by a factor of 3.

The geometrical characteristics of the the VG165 vortex generator configuration in RAE M2129 S-duct are given in Table 1. The results for flow at throat Mach number $M=0.66$ and Reynolds number based on mass flow and inlet radius $Re=0.39\times10^6$ are shown in Fig. 5, which depicts pressure recovery contours in the aerodynamic interface plane (AIP). The flow solution with fully gridded vortex generators is in Fig. 5a and with vortex-generator model for different model constant C_{VG} in Figs. 5b–5g. The sector pressure recovery in the 60-deg sector and DC_{60} index[19,20] vs radial angle of the sector in the AIP plane is shown in Fig. 6. The pressure recovery and DC_{60} index are evaluated from all points in the AIP plane. Both figures show that the solution is independent of the value of the model constant C_{VG} provided that its value is greater than or equal to $C_{VG}\geq7$. Even the results obtained with a model with constant $C_{VG}=5$ are still fairly accurate and predict well the tendency of the DC_{60} distortion index. Values of distortion index DC_{60} in the worst sector for the different model constants and their comparison to the DC_{60} from the fully gridded solution are given in Table 2.

Calculations were also carried out for the four different vortex-generator installations as defined in Anderson and Gibb[4] with the definition of geometrical characteristics given in Table 1. All four vortex-generator installations were simulated with the jBAY vortex generator model and with the same value of model constant $C_{VG}=10$ using the same grid. The pressure recovery on AIP plane along with smooth (baseline) configuration without vortex generators are shown in Fig. 7 and pressure recovery with pressure distortion in Fig. 8. The reduction of separation is clearly visible. The first installation VG130 is located downstream of the separation, that is, part of the vortex generator row lies inside the flow

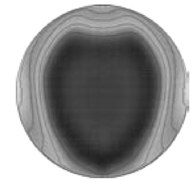

a) Fully gridded VG

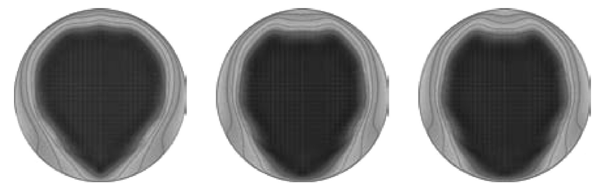

b) $C_{VG}=2$ c) $C_{VG}=5$ d) $C_{VG}=7$

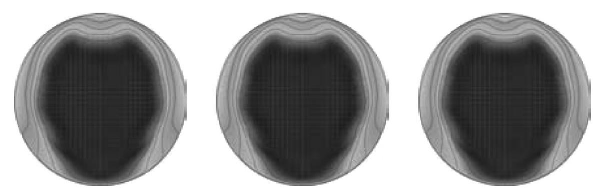

e) $C_{VG}=9$ f) $C_{VG}=10$ g) $C_{VG}=12$

Fig. 5 Pressure recovery in the AIP plane in flow through RAE 2129 S-duct, VG165 configuration, different model constants in jBAY vortex-generator model compared to the fully gridded vortex generators solution, $M_\infty=0.66$, $Re=0.39\times10^6$.

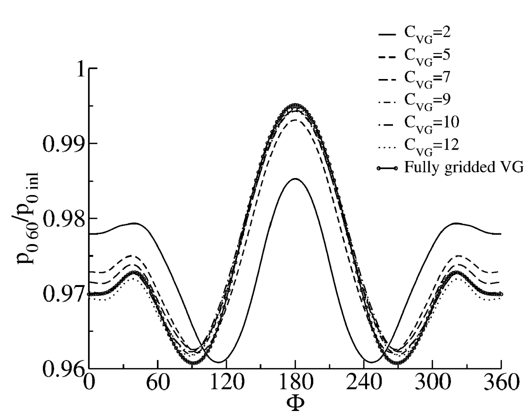

a) Pressure recovery

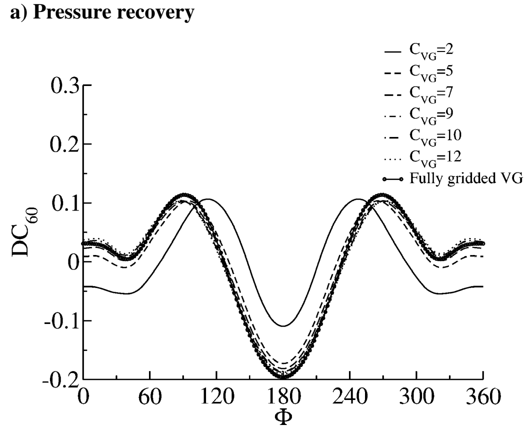

b) DC_{60} index

Fig. 6 Sector pressure recovery and pressure distortion in the AIP plane in flow through RAE M2129 S-duct, $M_\infty=0.66$, $Re=0.39\times10^6$.

a) Baseline

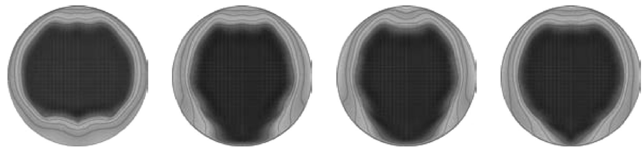

b) VG130 c) VG160 d) VG165 e) VG170

Fig. 7 Pressure recovery in the AIP plane in flow through RAE M2129 S-duct, four different VG configurations, solution with jBAY vortex generator model, $M_\infty = 0.66$, $Re = 0.39 \times 10^6$.

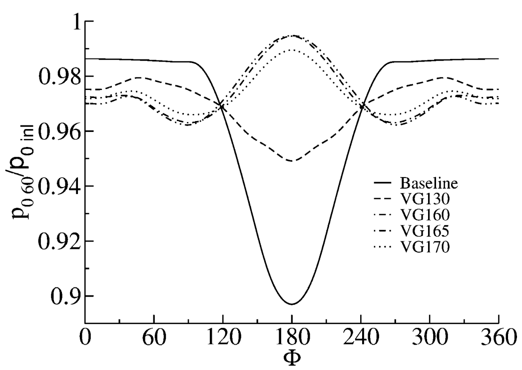

a) Pressure recovery

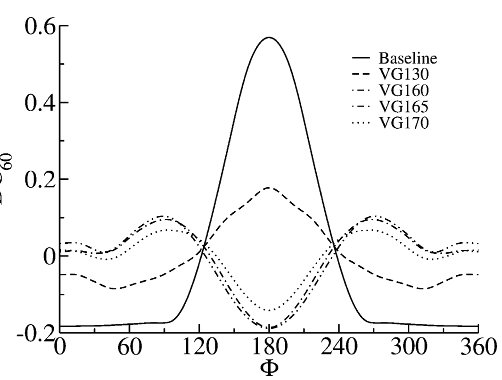

b) DC_{60} index

Fig. 8 Sector pressure recovery and pressure distortion in the AIP plane in flow through RAE M2129 S-duct, solution with jBAY vortex generator model, $M_\infty = 0.66$, $Re = 0.56 \times 10^6$.

separation region, which limits its effectiveness. However, even for this installation, the reduction of total pressure loss is still noticeable (Fig. 7b). Other three configurations shown in Figs. 7c–7e reduce separation completely.

C. Case 3: Three-Element High-Lift Airfoil with Vortex Generators

The third test case used to show the validation of the vortex generator model against the experimental data was the flow over a multi-element high-lift airfoil with vortex generators on the flap. The use of the vortex generators on a multi-element airfoil for reduction of flow separation has already been experimentally studied.[21,22]

This case was meant as a preliminary study of one of several possibilities along the path to the future design of more efficient high-lift devices.[†] The objective of the study is to reduce flap chord length, simultaneously increase main airfoil chord length and while keeping the same lift, reduce the weight of the entire device. The loss in lift, which is a consequence of flap size reduction, is compensated by allowing the higher deflection of the flap, which at higher angles of attack gives rise to the flow separation. This separation is then eliminated by employing a boundar-layer control, in this case by using a row of vortex generators.

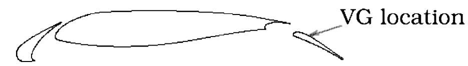

Fig. 9 Vortex-generator's location on the flap of high-lift airfoil.

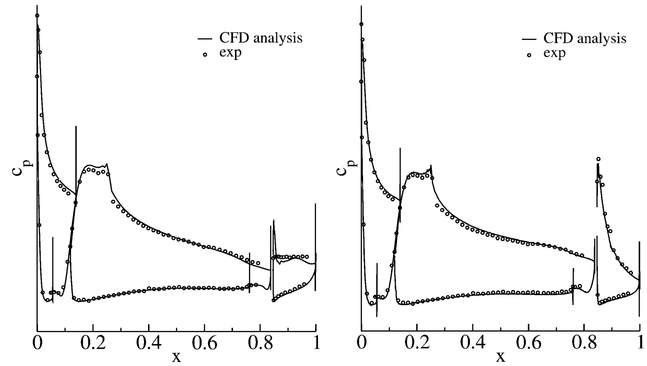

a) Without vortex generators b) With vortex generators

Fig. 10 The c_p coefficient on multi-element high-lift airfoil, solution with jBAY vortex-generator model, $M_\infty = 0.14$, $Re_\infty = 1.65 \times 10^6$, $\alpha_\infty = 18$ deg.

The row of corotating triangular vortex generators is located approximately at 25% of flap chord, as shown in Fig. 9 and consists of a number of corotating vortex generators of triangular shape with vortex generator height of the order of the boundary-layer thickness. The flow around the airfoil was measured at Mach number $M = 0.14$ and Reynolds number $Re = 1.65 \times 10^6$ at a sweep of angles covering the entire polar. Several angles of attack were calculated and compared to the experimental data. The result at one angle of attack $\alpha_\infty = 18$ deg is shown in Fig. 10. The value of the model constant was $C_{\mathrm{VG}} = 10$.

Figure 10 with c_p coefficient nicely shows the impact of vortex generators on the behavior of flow around high-lift configuration. The flow over smooth geometry (Fig. 10a) contains a large area of recirculating flow behind the flap, which is consequence of flow separation on the flap. In contrast, flow over high-lift airfoil equipped with vortex generators on the flap which is in Fig. 10b does not have any separation at all. Both adverse effects, separation and recirculation flow, were entirely eliminated by controlling boundary-layer behavior by vortex generators. The flow separation on the flap without vortex generators and its elimination by using vortex generators is clearly visible. The benefit of vortex generators is not limited only to the flap vicinity. Both the main airfoil and leading-edge flap are positively affected by increased circulation around the flap, and the entire device has higher lift than the one without vortex generators.

This case demonstrates both the ability of the vortex-generator model to accurately predict flow characteristics as well as an extreme efficiency of the application of vortex generators as a means of boundary-layer control.

V. Conclusions

An extension of the BAY vortex generator model, the jBAY model, has been developed and implemented into the Edge code. The jBAY vortex-generator model enables one to solve each vortex generator separately, is independent of vortex generator model constant C_{VG}, can model the vortex generators with different shapes and curvature, and is completely grid independent. The model requires minimal user input. The only existing limitation is that the model does not take into account the thickness of the vortex generator. However, for most applications this is not a problem because vortex

[†]Data available online at HELIX/TR/QinetiQ/C5.2/RL150803/2 [2003].

generators are usually very thin flat plates. The model is simple and can easily be implemented into existing codes.

The jBAY model has been tested on three very different cases: a flat plate with a single vortex generator, the RAE M2129 S-duct test with different vortex-generator installations, and a multi-element high-lift airfoil with vortex generators on the flap. The results were compared to a fully gridded analysis and to the available experimental data. In all cases the model gives results that show excellent agreement when compared to the fully gridded analysis or to the experimental data. The model uses one constant C_{VG} that is universal and does not have to be tuned for every case separately. The model's ease of use, simplicity in implementation as well as its high capability to reproduce or predict results, makes the model very attractive for use during computational-fluid-dynamics analysis.

Acknowledgments

Swedish Defence Materiel Administration Försvarets materielverk (FMV) is acknowledged for financing this project. Stephen Conway of Swedish Defence Research Agency FOI is gratefully acknowledged for making the structured grid around the vortex generator on a flat plate. The concept of vortex generator on a flap of a multi-element airfoil and data are originated in the EC 5th Framework programme HELIX, GRDI-2000-25205. This project was supervised by Simon Galpin of Airbus-UK. Ulf Tengzelius of FOI is gratefully acknowledged for providing the computational result of that computational-fluid-dynamics analysis. The author would like to express special thanks to Stephen Conway, Stefan Wallin, and Jonathan Smith of FOI for useful comments and revisions of this paper.

References

[1]Lin, J. C., "Review of Research on Low-Profile Vortex Generators to Control Boundary Layer Separation," *Progress in Aerospace Sciences*, Vol. 38, Nos. 4–5, 2002, pp. 389–420.

[2]Allan, B. G., Yao, C. S., and Lin, J. C., "Numerical Simulation of Vortex Generator Vanes and Jets on a Flat Plate," AIAA Paper 2002-3160, June 2002.

[3]Anderson, B. H., Yagle, P. J., Miller, D. N., and Traux, P. P., "A Study of MEMS Flow Control for the Management of Engine Distortion in Compact Inlet Systems," American Society of Mechanical Engineers, FEDSM99-6920, New York, July 1999.

[4]Anderson, B. H., and Gibb, J., "Vortex Generator Installation Studies on Steady State and Dynamic Distortion," *Journal of Aircraft*, Vol. 35, No. 4, 1998, pp. 513–520.

[5]Bragg, M. B., and Gregorek, G. M., "Experimental Study of Airfoil Performance with Vortex Generators," *Journal of Aircraft*, Vol. 24, No. 5, 1987, pp. 305–309.

[6]Lin, J. C., Robinson, S. K., McGhee, R. J., and Valerezo, W. O., "Separation Control on High-Lift Airfoils via Micro-Vortex Generators," *Journal of Aircraft*, Vol. 31, No. 6, 1994, pp. 1317–1323.

[7]Yao, C.-S., and Lin, J. C., "Flow-Field Measurement of Device-Induced Embedded Streamwise Vortex on a Flat Plate," AIAA Paper 2002-3162, June 2002.

[8]Bore, C. L., "Intakes for Vertical Landing Aircraft," *Practical Intake Aerodynamic Design*, edited by E. Goldsmith and J. Seddon, AIAA, Washington, DC, 1993, pp. 286–308.

[9]May, N. E., "A New Vortex Generator Model for Use in Complex Configuration CFD Solvers," AIAA Paper 2001-31014, June 2001.

[10]Kunik, W. G., "Application of a Computational Model for Vortex Generators in Subsonic Internal Flows," AIAA Paper 86-1458, June 1986.

[11]Bray, T. P., "A Parametric Study of Vane and Air-Jet Vortex Generators," Engineering Doctorate Thesis, College of Aeronautics, Flow Control and Prediction Group, Cranfield Univ., Shrivenham, U.K., 1998.

[12]Wendt, B. J., "Initial Circulation and Peak Vorticity Behavior of Vortices Shed from Airfoil Vortex Generators," NASA/CR-2001-211144, Aug. 2001.

[13]Bender, E. E., Anderson, B. H., and Yagle, P. J., "Vortex Generator Modelling for Navier–Stokes Codes," American Society of Mechanical Engineers, FEDSM 99-6919, New York, July 1999.

[14]Waithe, K. A., "Source Term Model for an Array of Vortex Generator Vanes," NASA/CR-2003-212157, March 2003.

[15]Eliasson, P., "EDGE, a Navier–Stokes Solver for Unstructured Grids," *Proceedings to Finite Volumes for Complex Applications III*, edited by D. Kroner and R. Herbin, Hermes Penton Science, London, 2002, pp. 527–534, URL: www.Edge.foi.se.

[16]Wallin, S., and Johansson, A., "A Complete Explicit Algebraic Reynolds Stress Model for Incompressible and Compressible Turbulent Flows," *Journal of Fluid Mechanics*, Vol. 403, 2000, pp. 89–132.

[17]Advisory Group for Aerospace Research and Development, "Air Intakes for High Speed Vehicles," AGARD, Advisory Rept. 270, Fluid Dynamics Panel Working Group 13, AGARD-AR-270, Sept. 1991.

[18]Anderson, B. H., Reddy, D. R., and Kapoor, K., "Study on Computing Separating Flows Within a Diffusion Inlet S-duct," *Journal of Propulsion and Power*, Vol. 10, No. 5, 1994, pp. 661–667.

[19]Aerospace Recommended Practise, "Gas Turbine Engine Inlet Distortion Guidlines," Society of Automotive Engineers, Inc., ARP 1420, Warendale, PA, March 1978.

[20]Seddon, J., and Goldsmith, E. L., "Distortion and Swirl," *Intake Aerodynamics*, 2nd ed., AIAA, Reston, VA, 1985, pp. 269–274.

[21]Lin, J. C., "Control of Turbulent Boundary-Layer Separation Using Micro-Vortex Generators," AIAA Paper 98-3404, July 1998.

[22]Rae, A. J., Galpin, S. A., and Fulker, J., "Investigation into Scale Effects in the Performance of Sub Boundary-Layer Vortex Generators on Civil Aircraft High-Lift Devices," AIAA Paper 2002-3274, June 2002.